Genome-Wide Loss of Heterozygosity and DNA Copy Number Aberration in HPV-Negative Oral Squamous Cell Carcinoma and Their Associations with Disease-Specific Survival

Chu Chen[1,2,3]*, Yuzheng Zhang[4], Melissa M. Loomis[1], Melissa P. Upton[5], Pawadee Lohavanichbutr[1], John R. Houck[1], David R. Doody[1], Eduardo Mendez[1,2,6], Neal Futran[2], Stephen M. Schwartz[1,3], Pei Wang[4,7]

1 Program in Epidemiology, Division of Public Health Sciences, Fred Hutchinson Cancer Research Center, Seattle, Washington, United States of America, 2 Department of Otolaryngology–Head and Neck Surgery, University of Washington, Seattle, Washington, United States of America, 3 Department of Epidemiology, University of Washington, Seattle, Washington, United States of America, 4 Program in Biostatistics and Biomathematics, Division of Public Health Sciences, Fred Hutchinson Cancer Research Center, Seattle, Washington, United States of America, 5 Department of Pathology, University of Washington, Seattle, Washington, United States of America, 6 Clinical Research Division, Fred Hutchinson Cancer Research Center, Seattle, Washington, United States of America, 7 Department of Genetics and Genomics Sciences, Mt. Sinai School of Medicine, New York, New York, United States of America

* cchen@fredhutch.org

Abstract

Oral squamous cell cancer of the oral cavity and oropharynx (OSCC) is associated with high case-fatality. For reasons that are largely unknown, patients with the same clinical and pathologic staging have heterogeneous response to treatment and different probability of recurrence and survival, with patients with Human Papillomavirus (HPV)-positive oropharyngeal tumors having the most favorable survival. To gain insight into the complexity of OSCC and to identify potential chromosomal changes that may be associated with OSCC mortality, we used Affymtrix 6.0 SNP arrays to examine paired DNA from peripheral blood and tumor cell populations isolated by laser capture microdissection to assess genome-wide loss of heterozygosity (LOH) and DNA copy number aberration (CNA) and their associations with risk factors, tumor characteristics, and oral cancer-specific mortality among 75 patients with HPV-negative OSCC. We found a highly heterogeneous and complex genomic landscape of HPV-negative tumors, and identified regions in 4q, 8p, 9p and 11q that seem to play an important role in oral cancer biology and survival from this disease. If confirmed, these findings could assist in designing personalized treatment or in the creation of models to predict survival in patients with HPV-negative OSCC.

Introduction

Oral squamous cell cancer (OSCC), which includes malignancies of the oral cavity and the oropharynx, proves fatal in many instances. The tumor and/or its treatment often lead to orofacial dysfunction and disfigurement. Oral cavity cancers are largely caused by tobacco and alcohol use, while infection with oncogenic Human Papillomavirus (HPV) often plays a role in the genesis of oropharyngeal cancer. Patients with HPV-positive oropharyngeal tumors generally have better treatment response and survival than do patients with HPV-negative oropharyngeal tumors. HPV status in oral cavity tumors does not seem to impact treatment response and survival. It is unclear whether this is a reflection of the underlying biology of oral cavity tumors, or rather because the low frequency of HPV-positive tumors in oral cavity cancer patients (reported to be 5–15%) has prevented a robust investigation. HPV-negative OSCC patients with tumors of the same clinical and pathologic stage have a heterogeneous response to treatment and likelihood of recurrence and survival. However, the molecular basis for this heterogeneity is also largely unknown.

Loss of heterozygosity (LOH) and DNA copy number aberration (CNA, defined as having an altered DNA copy number at a specific locus in the tumor compared to that in the peripheral blood leukocytes) that are associated with the inactivation of tumor suppressor genes (TSG) and the activation of oncogenes occur with various frequencies in squamous cell carcinoma of the oral cavity and oropharynx (OSCC) and other types of squamous head and neck cancer (HNSCC) [1, 2]. LOH and CNA patterns appear to differ at different points in the natural history of OSCC, and these patterns are, to some extent, correlated with clinical disease outcomes [3]. Furthermore, there is some evidence to suggest that LOH/CNA may be superior predictors of disease outcomes compared to the traditional TNM staging system [4, 5]. There is evidence that LOH on 2q, 3p, 6q25-27, 8p, 8p21.2, 8p23, 9p21-22, 10q, 11q23, 13q, 14q, 17p or 18q are associated with recurrence and/or poor survival of OSCC and/or HNSCC patients [6–9]. Other studies showed that DNA amplification, and DNA copy number gains and losses predict recurrence and/or survival of OSCC and/or HNSCC patients [6, 10–24]. Array CGH (aCGH) studies have reported that HPV-positive and HPV-negative HNSCC have both common and distinct CNA [25], and have also observed that gains and losses at various chromosome arms are associated with recurrence and/or length of survival [4, 5, 26, 27].

Although these efforts greatly advanced our understanding of genetic alterations relating to oral cancer, signal contamination caused by the presence of non-malignant cell populations, the low resolution, and the inability to identify balanced chromosomal changes such as copy-neutral LOH [28, 29] where LOH in one allele is compensated by the copy gain in the alternate allele in the paired chromosome, are the major limitations to the above mentioned studies. To improve upon these aspects in our efforts to identify potential chromosomal changes that may be associated with survival in HPV-negative OSCC, which accounts for the majority of OSCC worldwide, we interrogated paired peripheral blood DNA and DNA from tumor cells isolated by laser capture microdissection (LCM) using Affymetrix Human SNP Array 6.0 to examine the genome-wide landscape of LOH and CNA and to explore whether LOH and CNA are associated with OSCC-specific mortality.

Materials and Methods

Ethics statement

This work was conducted with written informed consent of study participants and was approved by the Institutional Review Offices of the Fred Hutchinson Cancer Research Center and the Veterans Puget Sound Healthcare System.

Study population

Eligible study participants were those who were $\geq$18 years of age, could communicate in English, were without prior treatment with radiation and/or chemotherapy, who underwent surgical resection or biopsy at the University of Washington Medical Center, Harborview Medical Center or the VA Puget Sound Health Care System in Seattle, Washington for their first primary OSCC between 2003 and 2010 [30]. Eligible participants were asked to donate tumor tissue and peripheral blood at or before the time of resection or biopsy. Tumor DNA was tested for HPV as previously described [31]. Participants were interviewed in person regarding demographic, lifestyle (including tobacco and alcohol use), medical, functional, and quality of life information. Tumor characteristics were obtained from medical records. Patients were followed actively through periodic telephone interviews to ascertain recurrence and changes in lifestyle characteristics, and passively through medical record reviews and linkages to the U.S. Social Security Death Index and the FHCRC's Cancer Surveillance System (one of NCI's SEER registries), which is updated semi-annually with the Washington State Death Certificate database and annually with the National Death Index. Classification of death as due to OSCC was based on information on the medical records and death certificates and independent adjudication by two otolaryngologists. This study was conducted with written informed consent and approvals by the Institutional Review Boards of the Fred Hutchinson Cancer Research Center, University of Washington and the VA Puget Sound Health Care System.

Isolation of tumor cells by laser capture microdissection (LCM)

Tumors retrieved from liquid nitrogen storage were embedded on dry ice using Tissue-Tek OCT Compound (Sakura Fineteck U.S.A., Torrance, CA) in 2-methylbutane. A 10-μm section was stained with hematoxilin and eosin for the pathologist (MP Upton) to identify regions rich in tumor. The same tumor-rich regions in successive sections were isolated by LCM using an Arturus^{XT} Microdissection System (MDS Analytical Technologies, Sunnyvale, CA) to yield enough tumor cells for 500 ng DNA for LOH/CNA detection.

Isolation of DNA from paired tumor cells and peripheral white blood cells

DNA from tumor cells was extracted using the Qiagen DNA Micro Kit; DNA from the white blood cells was isolated by salt precipitation [32]. The purity of DNA was high as judged by spectrophotometric A260 to A280 ratio of $\geq$1.8.

Interrogation of LOH and CNA using Affymetrix Genome-wide Human SNP Array 6.0

DNA samples were further processed per Affymetrix protocols and interrogated using the Affymetrix 6.0 SNP array. Affymetrix software tool and Genotyping Console 3.0.2 were used to determine signal intensities and whether samples passed the Affymetrix QC threshold of Contrast QC> 0.4 and a QC Call Rate>86%. The respective corresponding values for our 75 samples were 1.87 and >97.1%. Genotype calls were made using Birdseed v2 (Affymetrix Power Tools (APT), http://media.affymetrix.com/). Across the 19 replicate arrays of a reference sample assayed in different batches, ~98.8% of the probes had identical SNP calls. For quality control, we filtered out 3% SNPs that, in majority of subject DNA samples had poor APT confidence scores, or had high genotyping call discrepancy over the 19 reference arrays. To normalize raw allele intensity, we used the R package AROMA [33], which can adjust for allelic crosstalk, probe affinity, PCR fragment length and probe sequence effects. The Affymetrix.cel

files and associated patient characteristics can be found in the GEO database with Accession No.GSE68717.

Statistical methods for inferring LOH and CNA based on genotype calls and normalized probe intensities

We inferred the LOH status at each locus of each patient based on the genotype calls at that locus from the paired tumor and blood samples. We excluded any SNP that was homozygous in all tumors, which are non-informative to infer LOH, leaving 223,357 SNPs for further analyses. LOH positive loci may have copy number loss (CN $\leq$ 1), be copy number neutral (CN = 2) or show copy number gain (CN $\geq$ 3). LOH negative loci may also show copy number loss, gain, or neutrality. To determine the CNA segment, we used Parent/allele specific copy number estimation method (R package pscn [34]) which smoothes and estimates DNA copy number using maximizing likelihood and segments the results into regions with constant copy number. The 900K CNA probe data were thus downsized to 131K segments. Then based on the segmented data, we use the paired tumor and blood samples to estimate the FDR on CNV gain/loss calls in tumor samples at a given magnitude cutoff. Specifically, we assumed that there is no true copy number variation in the blood sample, and estimated FDR as the ratio of the number of probes surviving the cutoff in the blood sample versus that in the tumor sample. The final CNA gain/loss calls were made by controlling the FDR of the results at an average targeted level of 10% (the FDR across subjects ranged from 0 to 12%, with a median of 0.96%).

To assess the association between individual SNP's LOH/CNA status and patient survival, we focused on OSCC-specific death (n = 24) and employed a multivariable Cox regression model adjusting for age, sex, and smoking history to evaluate the strength of the associations. The association of LOH/CNA events with OSCC-specific survival was determined with hazard ratios (HRs), and the corresponding 95% confidence intervals (CIs). There are possible models including univariate model with CNA only, univariate model with LOH only, multivariate model with both CNA and LOH, and the full model with CNA, LOH and a term representing the multiplicative interaction of CNV and LOH (CNA*LOH). Sex, age and smoking status were included in all the above models. We conducted the log-likelihood ratio test comparing the full model and the nested model to find out the significance of association. To account for multiple hypotheses testing, we further estimated False Discovery Rate using the R package q-value [35].

Results

We generated genome-wide LOH and CNA data on 75 patients with first, newly-diagnosed HPV-negative OSCC. S1 Table shows selected characteristics of these patients who were mostly white, male, current smokers and alcohol drinkers. The median follow-up was 75.7 months in patients alive at last follow-up (range 32.7–111.4), and 46.9 months (range 1.1–111.4) for all 75 patients. About 58.7% had late stage (AJCC stage III & IV) OSCC and 46.7% had lymph node involvement. Forty patients were deceased as of March 2014, among whom 24 patients had died of OSCC.

Genome-wide LOH events and copy number gains/losses in tumor tissue

The percentage of samples showing LOH at each probe from autosomes ranged 0%-90% (mean ± sd: 14.2 ± 13.3%) (Fig 1A). Frequent LOH events (appearing in >20% of the samples) were observed in all autosomes. Some segments on 3p and 9p along with one SNP in 8q24
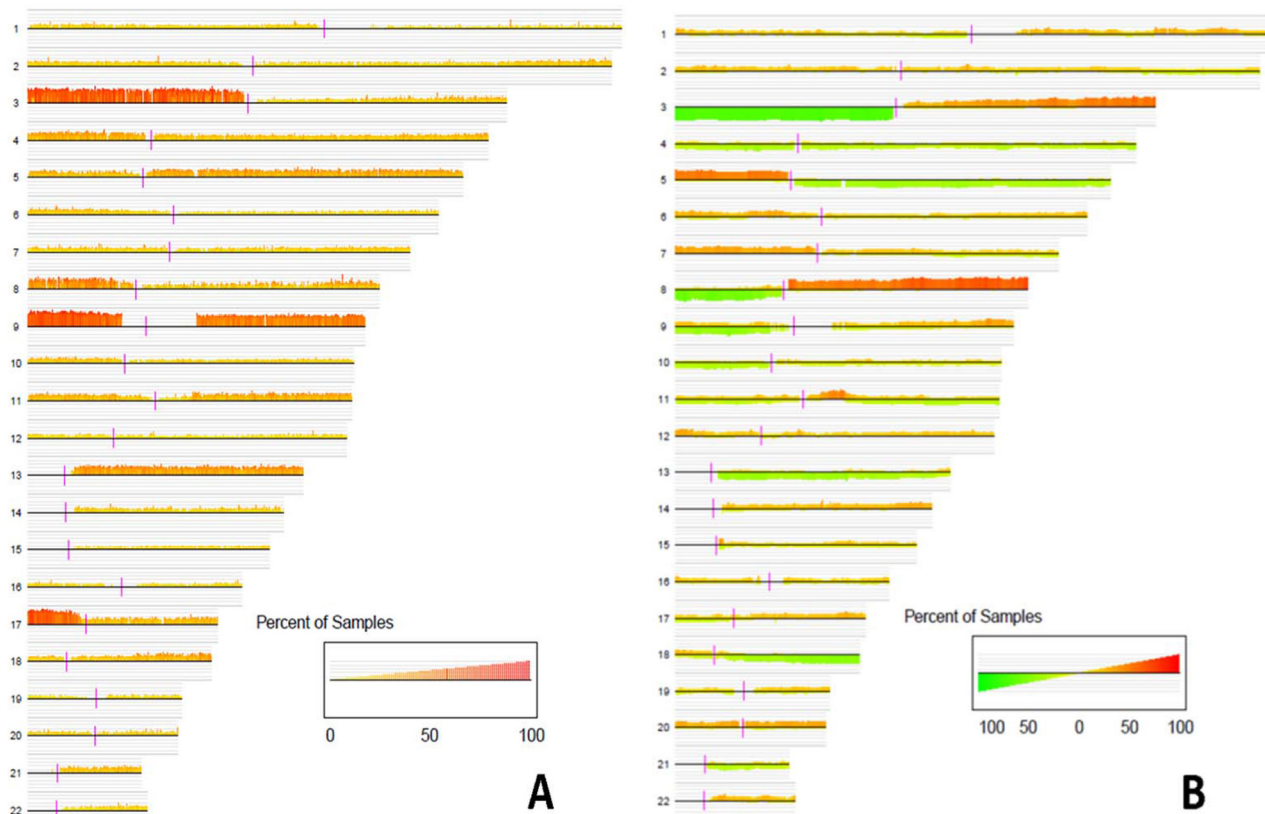
Fig 1. Consensus plot of genome-wide LOH events. (A) and copy number gains and losses (B) for each autosome. The height and the color of the vertical lines represent the percentage of samples in which the corresponding probes have LOH (A) or copy number gains (red)/losses (green) (B). Horizontal gray lines indicate percentages ranging from 0, 20%, 40%, 60%, 80% to 100% The p arm (left) and q arm (right) in each chromosome are delineated by a vertical purple bar.

doi:10.1371/journal.pone.0135074.g001

(rs16904097) and one SNP in 17p (rs2042004) exhibit extremely frequent LOH (in >80% of samples) (Fig 1A). The region on Chr. 9p with extremely frequent LOH contains 30 SNPs, corresponding to eight genes (*FLJ35024, KDM4C, CCDC171, IL33, PTPRD, TTC39B, SH3GL2, FREM1*) and 15 inter-genic positions (rs1947447, rs10976390, rs1538718, rs10757623, rs7864275, rs4512431, rs1328001, rs10967005, rs10733410, rs4740766, rs12346508, rs726353, rs10125418, rs2375075, rs882092, rs10811970) within 9p21.2-9p24.3. The neighboring region of these 30 SNPs harbor several known TSG, including *p16/CDKN2* gene cluster, *TUSC1, SH3GL2* and *DMRT2*, which also exhibit frequent LOH events: one SNP in *p16* showed LOH in 37% of the samples; 20 SNPs in *SH3GL2* showed LOH in 36% of the samples, and one SNP in *DMRT2* showed LOH in 41% of the samples. The respective top 100 SNPs showing the most frequent LOH (including copy number gain LOH copy number loss LOH and copy number neutral LOH), DNA copy number gain, and DNA copy number loss are listed in S2 Table.

Frequent copy number gain events (appearing in >20% of the samples) were observed in 20 autosomes (except Chr. 4 and 21, Fig 1B); while frequent copy number loss events (similarly defined) were observed in 14 autosomes (except Chr. 1, 6, 7, 12, 16, 19, 20, 22). Among oncogenes and TSG that have been implicated in HNSCC, we found copy number gain and loss of *EGFR* (36% and 1.3% of the samples, respectively), *ERBB2* (21.3% and 4% of the samples, respectively), *FAT1* (5.3% and 27% of the samples, respectively), *SMAD4* (1.3% and 41% of the samples, respectively); and *CDKN2A* (8% and 54.7% of the samples, respectively).
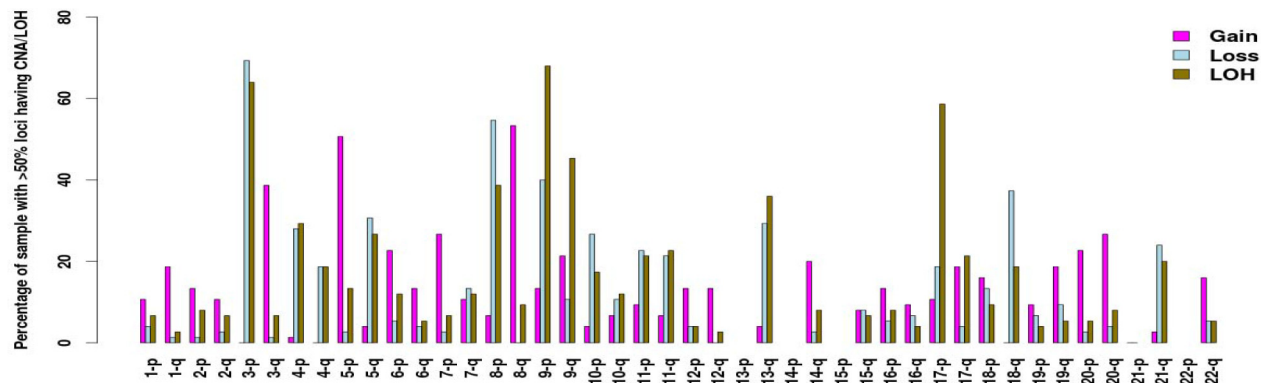
Fig 2. Percentage of OSCC having large-region-gain/loss/LOH for each chromosome arm. Large-region-gain/loss/LOH is defined as gain/loss/LOH events occurring at more than 50% of probes of one chromosome arm in a sample.

Percentage of probes in 22 autosomes showing CNA and LOH events varies among different samples (S1 Fig). The percentage of probes showing LOH in each sample ranges 0.33% to 43% (mean ± sd: 14.19 ± 10.75%). The percentage of probes showing CNA in each sample ranges from 0.03% to 82.6% (mean ± sd: 30.1% ± 18.4%). Copy number gain events range from 0% to 52% (mean ± sd: 17.1% ± 11.6%); copy number loss ranges from 0% to 33.9% (mean ± sd: 13 ± 9.1%). Tumors with more LOH also are more likely to have more CNA.

Chromosome arms 3p, 8p, 9p, 9q, 13q and 17p contain *large-region-LOH* events, as defined by having more than 50% of probes on the chromosome arm showing LOH, in at least 27 of the 75 samples (36%) (Fig 2). Similarly, frequent *large-region-gain* was seen for 3q (38.7% of the samples), 5p (50.7%), and 8q (53.3%), and frequent large-region-loss was seen in 3p (69.3%), 8p (54.7%) and 9p (40%).

Association of genome-wide LOH/CNA events with tumor characteristics, lifestyle factors and OSCC-specific mortality

We clustered samples into two groups using genome-wide autosome CNA and LOH events and examined the association between the resulting clusters and tumor characteristics, OSCC-specific mortality and two major OSCC risk factors (cigarette smoking and alcohol use). The genome-wide hierarchical clustering on CNA/LOH events did not reveal associations with tumor characteristics or mortality (S3 Table, S2 Fig for CNA; S3 Fig for LOH). However, LOH clusters showed a statistically significant difference in smoking status (S3 Table, Fisher Exact test p = 0.0069).

Association of CNA/LOH at specific genome regions with tumor characteristics and OSCC-specific mortality

For CNA, we focused on regions with high-level copy number amplification (defined as the difference between estimated copy number in the tumor sample vs. that in the matched blood sample being ≥5) (Fig 3A). Two regions on Chr. 11 (Fig 3B) have frequent high-level copy number amplification; region 1: 11q13.1–14.3, nt68683098 to nt70375682, with CNA≥5 observed in *MYEOV, CCND1, ORAOV1, FGF19, FGF4, FGF3, ANO1, FADD, PPF1A1, CTTN* and *SHANK2*; and region 2: 11q22-24, nt99440128 to nt102804260, with CNA≥5 observed in MMP-1, -3, -7, -8, -10, -12, -13, -20, and -27; *ARHGAP42; YAP1; TRPC6; CNTN5; DYNC2H1; TMEM123; WTAPP1; LOC10105; BIRC3; KIAA1377; C11orf70; DCUN1D5; PGR;* and *ANGPTL5.* The percentages of samples showing high-level CN amplification in these two
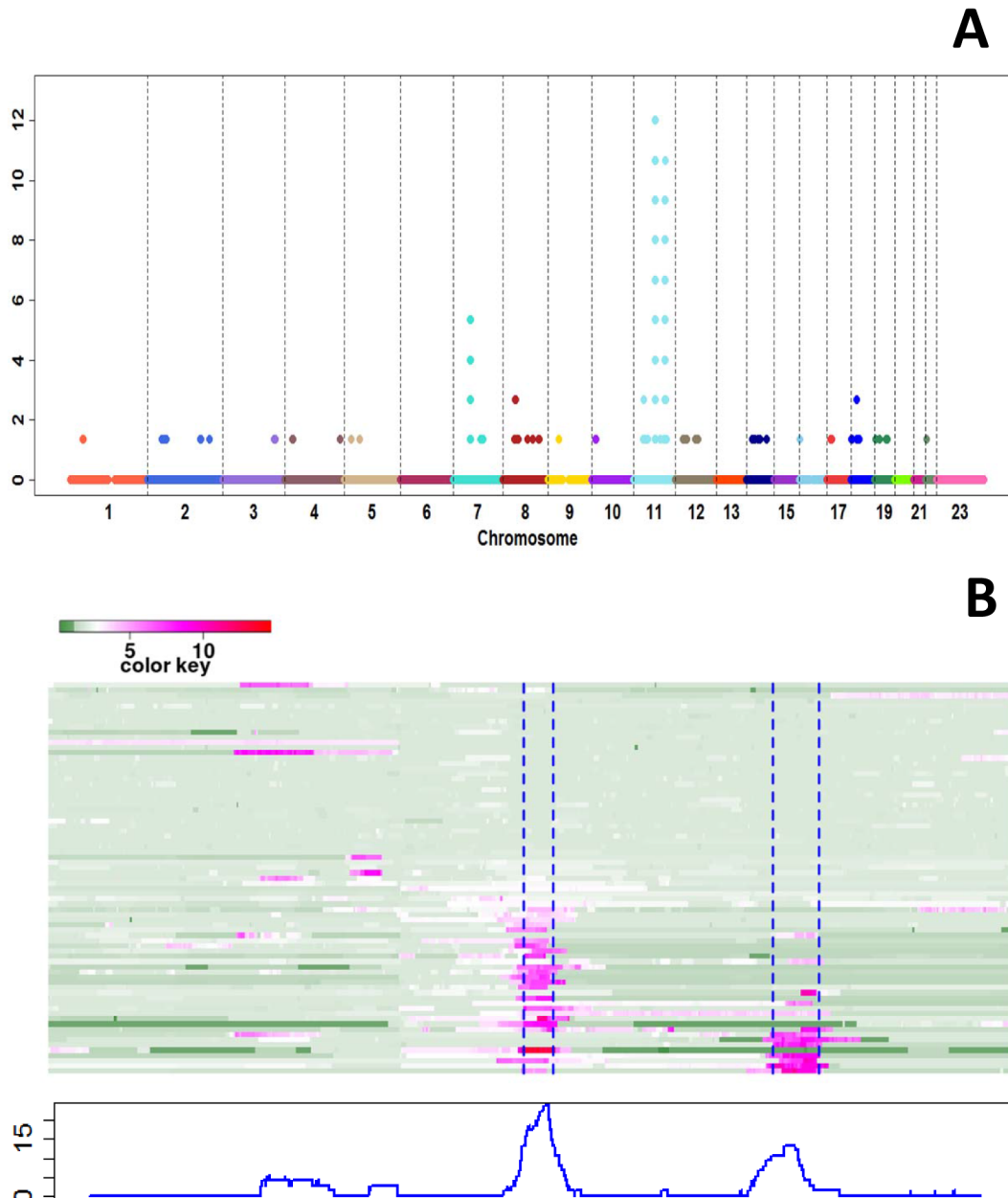
Fig 3. Results on copy number amplification. A) High-level copy number amplifications. Each dot represents one probe. *X-axis*: genome order of probes from 22 autosomes. *Y-axis*: Percentage of samples showing high copy number amplification at each probe. High copy number amplification is defined as the difference between copy number in a tumor sample vs. that in the corresponding blood sample being greater than or equal to 5. B) Chromosome 11 tumor copy number data. The top panel shows the heatmap of tumor CN data with probes in columns and 75 subjects in rows. The blue dashed lines label the high-level amplification regions 1 and 2. The bottom panel shows the percentage of samples having high-level copy number amplifications (CNA> = 5) at each probe.

doi:10.1371/journal.pone.0135074.g003

regions are approximately 20% and 10%, respectively (Fig 3B). Heatmaps illustrating the LOH and CNA data of these two regions are shown in Fig 4 and S4 Fig, respectively. Interestingly, while 8–29% of the study participants have LOH in region 1, most of the copy number gain events in region 1 are also accompanied with LOH (Fig 4). Applying hierarchical clustering on CNA data in this region further divided the patients into two major groups: 23 patients with numerous copy-number-gain-LOH events; and 52 with few LOH or CNA events (Fig 4 left top
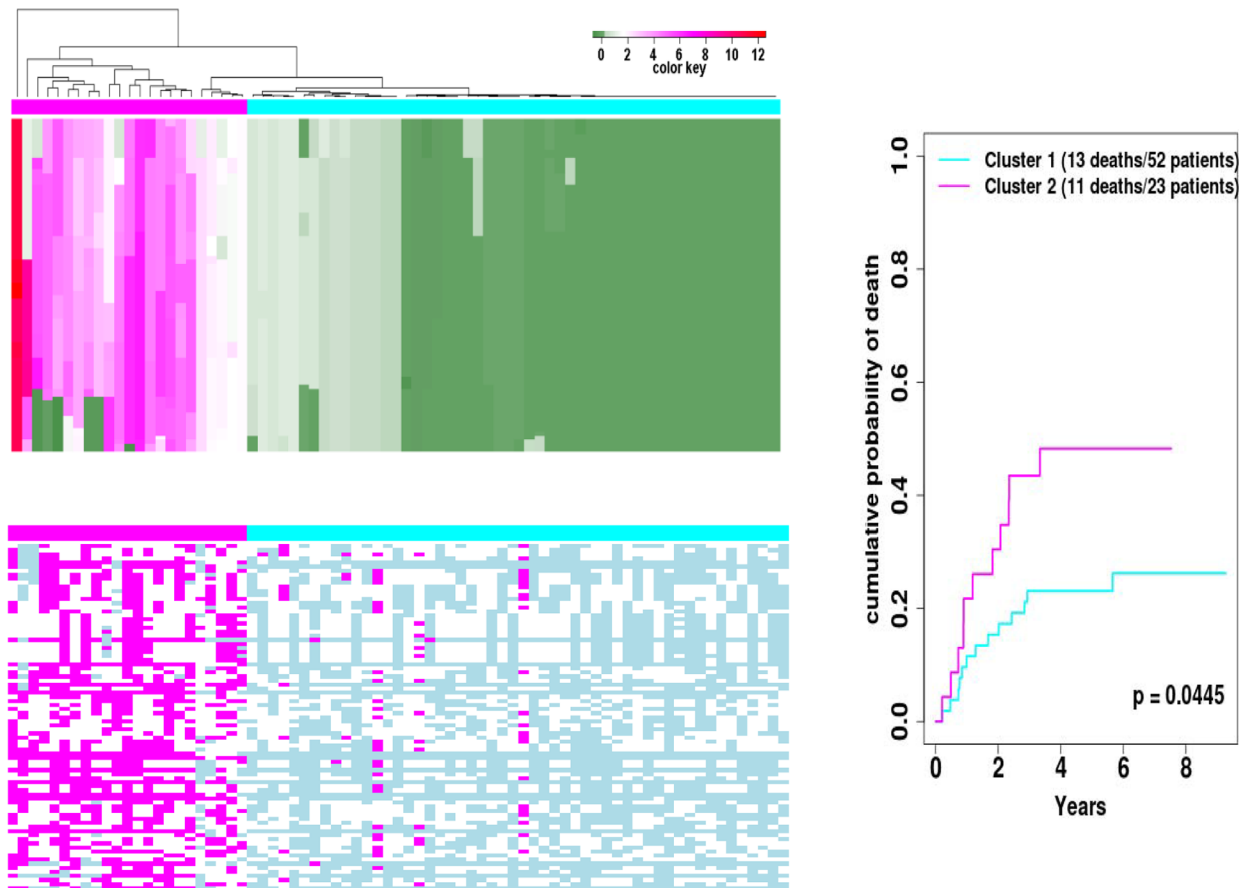
Fig 4. CNA and LOH data for the high-level amplification region 1 in 11q 13.1–14.3 (85 probes from nucleotide position nt68683098 to nt70375682). The top left panel shows the heatmap of tumor CNA data, and the color key indicates the estimated copy number. The bottom left panel shows the heatmap of LOH data (magenta, LOH present; blue, no LOH; white, not informative). In both heatmaps, the rows stand for SNPs and the columns stand for samples. Based on the CNV data, we clustered the samples into two groups (23 patients in the magenta group and 52 patients in the blue group) using hierarchical clustering algorithm. The right panel shows the cumulative incidence curves of the OSCC-specific death of the patients in the two clusters. The X-axis indicates the years between surgery and last follow-up or death. The Y-axis indicates the cumulative incidence of death due to OSCC. OSCC-specific mortality of the two clusters of patients was significantly different (p = 0.0445) according to log rank test.

doi:10.1371/journal.pone.0135074.g004

panel). Cumulative incidence analyses indicate that the group of 23 patients had a greater likelihood of OSCC-specific mortality (log rank test p = 0.0445 comparing 11 deaths of 23 patients vs. 13 deaths of 52 patients, Fig 4, right panel). Patients in these two groups do not appear to differ by TNM staging, tumor site and history of tobacco smoking and alcohol use (S4 Table). When the patients were clustered into two groups based on their LOH events in this region, the cumulative incidence curves did not show a statistically significant difference between the two groups (data not shown). When hierarchical clustering on CNA data in region 2 subdivided the patients into two subgroups, no statistically significant difference in OSCC-specific mortality between the subgroups was observed (S4 Fig). There was a small suggestion that CNA events in this region might be related to history of tobacco use (S4 Table, Fisher Exact test p = 0.067). There were greater percentages of smokers, especially current smokers, than non-smokers in cluster 1, which had fewer CNA events than cluster 2; the percentages of current, former and never smokers were 48%, 36% and 16%, respectively. Current and former smokers were less likely than non-smokers to be in cluster 2, which had greater number of CNA events; the respective percentages of current, former and never smokers were 23%, 31%
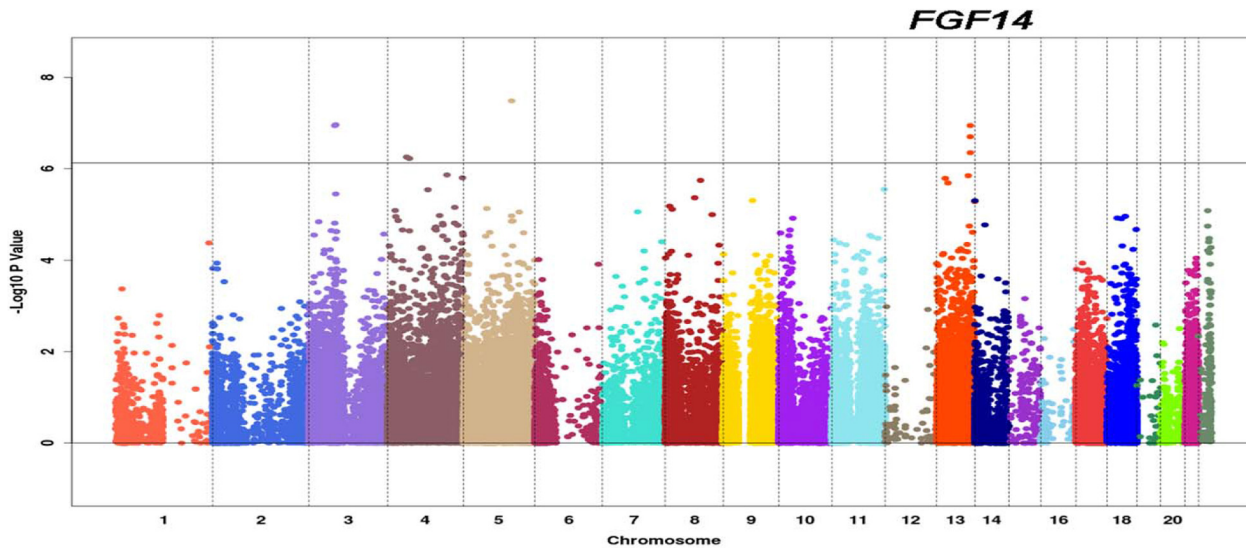
Fig 5. Manhattan plot of p-values for testing interaction effects between each probe's LOH status and its DNA copy number in Cox regression models for OSCC-specific survival. The X-axis shows the genome order with different chromosomes separated by vertical dashed grey lines. The Y-axis shows the negative $\log_{10}$ p-values from log-likelihood ratio test for testing the interaction term (CNV*LOH) in the Cox model that included terms for sex, age, and smoking history. The horizontal grey line corresponds to Bonferroni cutoff 0.05/66875.

and 46%. Thus, these results suggest that smokers are less likely to have abnormal CNA in region 2.

For LOH, we focused on Chr. 9p (Fig 2), which has the most frequent *large-region-LOH* in this data set. The two clusters of patients defined by LOH frequencies on this chromosome arm, with cluster 2 harboring more LOH events, differed significantly in terms of their smoking history (S5 Table, p = 0.002). Patients in cluster 2 were more likely to be smokers, especially current smokers; the respective percentages were 57%, 29% and 14% for current, former and never smokers. These results suggest that tobacco exposure may result in a large number of LOH events on Chr. 9p. No statistically significant differences were detected between two groups' cumulative probability of OSCC-specific mortality (S5 Fig, p = 0.782).

Association of individual SNPs with OSCC-specific mortality

Cox regression models were fit to assess the association between OSCC-specific mortality and CNA or LOH of each probe, as well as their interaction, adjusting for sex, age and smoking. After filtering out probes with LOH events occurring in fewer than 5 samples, there were 66,875 probes considered in the analysis. The Manhattan plots in Fig 5 and Fig 6A show the-$\log_{10}$(p value) from the likelihood ratio tests for the interaction effect between CNA and LOH of each SNP, and the overall contribution of each SNP's CNA and LOH information in the Cox regression, respectively. There were eight probes for which the interactions between CNAs and LOHs appear to be statistically significant in their Cox models based on Bonferroni corrected significance level of 0.05 (p-value <7.48e-07) (Fig 5, Table 1). Among the eight probes, three have complimentary sequence to *FGF14*. The corresponding results shown in Table 1 suggest an interesting modifying effect of LOH on the association between CNA of *FGF14* and mortality in that copy number gains of this gene increase the hazard rate in those patients with LOH at this gene (positive lnHR), while decrease the hazard rate in those patients without LOH (negative lnHR).
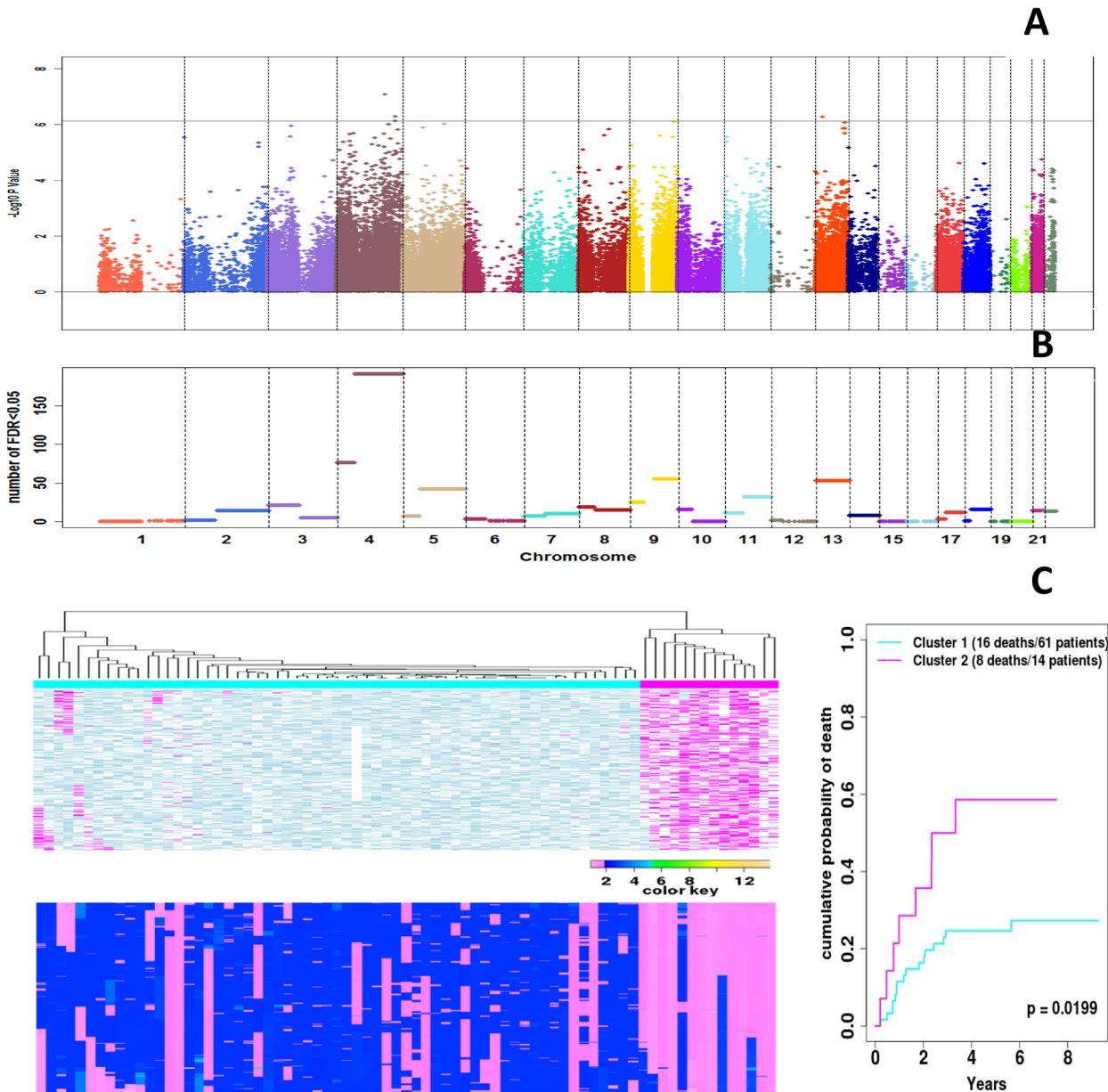
Fig 6. Association of each probe's LOH status and DNA copy number with OSCC-specific mortality. A) Manhattan plot of p-values for testing the association of each probe's LOH status and DNA copy number with OSCC-specific mortality. The X-axis shows the genome order with different chromosomes separated by vertical grey lines. The Y-axis shows the negative $\log_{10}$ p-values from likelihood ratio test for testing the main effect and interaction terms for CNV & LOH in the Cox model that also include terms for sex, age, and smoking history. The horizontal grey line corresponds to Bonferroni cutoff 0.05/66875. B) Number of loci in each chromosome arm, whose p-value survived the FDR 0.05 cutoff in A). The X-axis again stands for the genome order. The Y-axis stands for the number of probes (probes from the same chromosome arm share the same value). C) LOH and CNA data for the whole Chr. 4q (8975 probes from nucleotide position from 63637813 to 183550869). The top left panel shows the heatmap of LOH data (magenta, LOH present; blue, no LOH; white, not informative). The bottom left panel shows the heatmap of tumor CN data, and the color key indicates the copy number. In both heatmaps, the rows stand for SNPs and the columns stand for samples. Based on the LOH data, we clustered the samples into two groups (14 patients in the magenta group and 61 patients in the blue group) using hierarchical clustering algorithm. The right panel shows the Cumulative Incidence curves of the OSCC-specific death of the patients in the two clusters. The X-axis indicates the years between surgery and last follow-up or death. And the Y-axis indicates the mortality rate. Survival of the two clusters of patients was significantly different (p = 0.0199) according to log rank test.

doi:10.1371/journal.pone.0135074.g006

For each SNP, we tested the joint effect of LOH, CNA and their interaction term in the Cox models. We found four probes (with one each corresponding to *PALLD*, *DDX60L* and

Table 1. Eight probes with statistically significant interaction effects between CNA and LOH on OSCC-specific mortality.

Cyto-band	SNP ID	RS position	Gene Symbol	Nucleotide position	p.all[†]	p.CNA*LOH[††]	Direction of CNA association	
							No LOH	LOH present
3p26	SNP_A-2231666	rs4478080	FAM19A1	68320588	1.12E-06	1.09E-07	*	+
3p26	SNP_A-8591805	rs2060023	MAGI1	65974572	2.71E-06	1.13E-07	*	+
4q12	SNP_A-1855888	rs17750221	—	55040244	9.91E-06	5.95E-07	+	-
4p12	SNP_A-2196903	rs7694862	TEC	48190372	2.11E-06	5.54E-07	*	-
5q35	SNP_A-1806221	rs4343835	SNX2	122116630	9.44E-07	3.27E-08	-	+
13q34	SNP_A-2182075	rs951348	FGF14	102788188	2.08E-06	4.44E-07	*	+
13q34	SNP_A-4289264	rs952645	FGF14	102787731	8.74E-07	1.13E-07	-	+
13q34	SNP_A-8316408	rs7994713	FGF14	102789615	1.40E-06	1.99E-07	-	+

‡ p-values from the log-likelihood ratio test for terms for CNA, LOH, and the multiplicative interaction of CNA and LOH (LOH*CAN) in the Cox regression model.

‡‡ p-values from the log-likelihood ratio tests of the interaction term (cnv*loh).

* Direction of association undetermined.

doi:10.1371/journal.pone.0135074.t001

MAML3) significantly associated with OSCC-specific mortality with the Bonferroni corrected p-values <0.05 (Fig 6A, Table 2). Results in Fig 6A also suggest that there are a large number of probes on Chr. 4 showing moderate association (low p-values). Indeed, at FDR = 0.05, we find 675 SNPs showing significant association with OSCC deaths. Among these, a large percentage (28.3%) is on Chr. 4q (Fig 6B). This motivated us to assess the connection between LOH/CNA of this chromosome arm and mortality. We clustered patients into two groups (14 vs. 61) based on LOH on 4q. Patients in the two clusters were similar in tumor size, site, nodal status, smoking and alcohol use history, but differ by AJCC stage (S6 Table, Fisher Exact test p = 0.0477). Cumulative incidence curves of OSCC-specific mortality of these two groups showed a statistically significant difference (Fig 6C, log rank test p = 0.0199). Furthermore, the two LOH-based clusters show significantly different association with patients' mortality even when AJCC stage was included in the adjustment (log-likelihood ratio test p = 0.00161). We

Table 2. List of 4 probes of whom the combined information of CNA and LOH are significant for predicting OSCC-specific m.

Cyto-band	SNP ID	RS position	Gene Symbol	Nucleotide position	P (CNA, LOH, & CNA*LOH terms)‡	P (CNA*LOH Interaction)‡‡	Direction of CNA association	
							No LOH	LOH present
4q33	SNP_9242309	rs12647997	PALLD	169663775	7.47E-07	0.63	*	+
4q33	SNP_A-8393999	rs9685229	DDX60L	169371116	5.26E-07	1.54E-05	+	+
4q31.1	SNP_A-8706233	rs11100449	MAML3	141171560	8.53E-08	4.15E-03	*	+
13q14	SNP_A-2115691	rs7339301	—	39637333	5.42E-07	1.62E-06	-	+

‡ p-values from the log-likelihood ratio tests for the combined term (cnv+loh+cnv:loh) in the cox regression model "OSCC-specific survival ~ CNV + LOH + CNV:LOH + sex + age +smoking history".

‡‡ p-values from the log-likelihood ratio tests of the interaction term (cnv:loh).

* Direction of association undetermined.

doi:10.1371/journal.pone.0135074.t002

conducted the same analysis using CNA data of 4q, but didn't detect a significant difference in their association with OSCC-specific mortality (S6 Fig).

Discussion

This study used LCM isolated tumor cells from fresh frozen tumor samples and paired peripheral blood leukocytes and the high density Affymetrix Genome-wide Human SNP Array 6.0 to interrogate LOH/CNA events in HPV-negative OSCC and their association with OSCC-specific mortality. It detected a wide array of LOH and CNA events among tumors from 75 patients. All tumors harbored LOH and/or CNA, with no two exhibiting the same LOH/CNA patterns on the genome-wide level.

This study confirms and adds to previous evidence regarding LOH and CNA in certain chromosomal regions and gene loci that may play an important role in oral cancer biology and prognosis. The observation of frequent LOH events on Chr. 3p, 9p, 11q and 17p is consistent with previous reports [6, 36–61]. A number of genes on Chr. 3p have been proposed to be HNSCC TSG that are shared with breast or colon cancer [62]. Based on the respective top 100 SNPs exhibiting the most frequent LOH or copy number loss in our study, the potential TSG on Chr. 3p would include *TGFBR2*, *CNTN4*, and *CHL1* (reported for colorectal cancer) and *CNTN6* (for breast cancer [63]), as well as *FHIT*, *ROBO1-GRE1* and *SETMAR-LRRN1*. So far, few studies have proposed HNSCC TSG in Chr. 9p [44]. Our results on extremely frequent LOH (in >80% of patients tested) suggest that eight genes (*FLJ35024*, *KDM4C*, *CCDC171*, *IL33*, *PTPRD*, *TTC39B*, *SH3GL2*, *FREM1*) within Chr. 9p21.2–24.3 may be TSG for HNSCC that, with the exception of *PTPRD and SH3GL2*, have not been recognized previously. *KDMC4* is a histone demethylase involved in chromatin remodeling [64, 65]. IL33 expression has been reported to be elevated in HNSCC and may promote cell migration and invasion [66]. *PTPRD* encodes for a phosphatase that regulates cell cycle. Its inactivation via homozygous deletion and/or mutation has been reported in several cancers, including HNSCC [67–69]. Our finding adds to the reported mechanisms of its inactivation. Variant genotypes of *TTC39B* have been associated with dyslipidemia [70, 71]. The present study is the first to implicate it in cancer and raises the question of what role lipid metabolism may play in OSCC pathophysiology. There is some prior evidence to support *SH3GL2* as a HNSCC TSG in that its decreased expression and/or deletion was associated with laryngeal cancer [72, 73]. The current study is the first to suggest its potential role as a TSG in OSCC, and that LOH may be another mechanism for its dysregulation. *FREM-1* encodes for an extracellular matrix adhesion protein [74]. The current study is the first for its implication in cancer. Further human and model system studies to verify our new findings implicating *KDM4C*, *PTPRD*, *TTC39B*, *SH3GL2*, *FREM1* as potential TSG are warranted. It is noteworthy that at least for the top 100 SNPs associated with the most frequent LOH, the LOH events were accompanied by copy number gain, loss, or neither gain nor loss, attesting to the complexity of genomic changes in OSCC. It is also notable is that the top 100 SNPs with copy number gains are all in 8q24. The genes harboring these SNPs (S1B Table) could be potential oncogenes for OSCC and warrant further investigation.

Our observed DNA copy number gains of oncogenes *EGFR* and *ERBB2* and copy number loss of TSG *CDKN2A* and *SMAD4* are consistent with prior reports on HNSCC [6, 75–84]. *FAT1* encodes for a cadherin protein implicated in the adhesion and migration of oral cancer cells [85]. Results from the Cancer Genome Atlas project [86] and the India Project conducted by the International Cancer Genome Consortium (India project team of the International Cancer Genome Consortium, 2013) showed that *FAT1* is mutated in 20%-40% of HNSCC. Homozygous loss of *FAT1* has been reported in a study of oral cancer [87]. Based on its frequent

mutations and copy number loss in cancer, *FAT1* has been hypothesized as a TSG. Our results showing copy number loss in *FAT1* adds support to this hypothesis.

Amplification of 11q13.1–14.3 region in HNSCC has been observed by others [6, 84, 88–96]. Our observation of high-level copy number amplification of *MYEOV, CCND1, ORAOV1, FGF19, FGF4, FGF3, ANO1, FADD, PPF1A1, CTTN* and *SHANK2* in this region is consistent with prior reports and supports the hypothesis that they might be oncogenes and warrants further investigation into their potential as therapeutic targets. Our observation that the majority of patients who harbor high copy number amplification in this region also have LOH events and that patients with copy-number-gain-LOH in this region have poorer survival than those who rarely have CNA or LOH in this region represents a new discovery and requires further validation. The fact that patients clustered by CNA rather than LOH showed a significant difference in OSCC-specific mortality underscores the importance of gene amplification in this region and the need to investigate the amplified genes in their role as potential drivers for OSCC aggressiveness, prognostic indicators, and targets for therapeutic intervention.

Our results showed that region 2 of Chr. 11q (11q22-24) also contains many genes with high level of amplification (CNA≥5), including many MMPs (MMP-1, -3, -7, -8, -10, -12, -13, -20, and -27). This observation underscores the pivotal function of metalloproteinases in OSCC progression. High level of amplification of *MMP-1, -3, -7,-10,-12, -13* in HNSCC has previously been reported [97], while amplification of *MMP-8, -20*, and *-27* has not. *ARHGAP42* is a RhoGTPase activating protein. No prior reports linking it to cancer. Others have hypothesized *YAP1* to be a driver gene for HNSCC [98–100]; our observed high level *YAP1* amplification lends support to this hypothesis. High *TRPC6* expression has been observed in other cancers [101–105] and was reported to be associated with poor prognosis of esophageal cancer [105]. *CNTN5* encodes an adhesion molecule that mediates cell surface interactions during neural development. Our finding is the first to link *CNTN5* with cancer. Whether it plays a role in perineural invasion by participating in reciprocal signaling between nerves and OSCC as demonstrated by plexins and semaphorins in HNSCC models [106] warrants examination. *DYNC2H1* encodes a dynein protein purported to be involved in immune system and cytoskeleton remodeling. *TMEM123* encodes a transmembrane maturation marker for dendritic cells in mice [107]. *WTAPP1*, a pseudogene with unknown function, has been reported to be associated with Wilms' tumor. Amplification of *BIRC3* has been reported in acute myeloid leukemia [108] and pancreatic cancer [109]. Little is known about *KIAA1377*. *DCUN1D5* encodes for a protein involved in neddylation of cullin. Its overexpression was reported in laryngeal cancer [110]. *ANGPTL5* encodes for angiopoietin-like 5 protein that supports the engraftment of human hematopoietic stem cells in NOD-SCID mice [111]. Our results showing high copy number of this gene in OSCC is the first to implicate its role in carcinogenesis.

We observed that copy number gains of *FGF14* are associated with an increased risk of OSCC-specific mortality in patients with LOH in this gene, and a decreased risk in patients without LOH. This observed interaction effect between LOH and CNA suggests that the two alleles might involve very different functional consequences. Such phenomenon can be detected only when both LOH and CNA information are available–a strength of our study. While interesting, these findings need to be interpreted with caution and validated in larger populations because the sample size of this study is still quite limited. Dysregulation of FGF signaling in cancer and FGFs' potential as therapeutic targets are active areas of research [112–115]. While having sequence homology to FGFs, FGF14 does not activate FGF receptor as a true ligand [116]. Instead, it was found to be an intracellular modulator of voltage-gated sodium channel essential for regulating neuronal activities [117]. It would be of interest to examine the biological function of FGF14 in oral carcinogenesis and whether its expression is in anyway related to perineural invasion of OSCC.

Our results showed that CNA, LOH, and their interaction for a probe in each of *PALLD*, *DDX60L* and *MAML3* genes were significantly associated with OSCC mortality. *PALLD* *encodes* palladin, an actin-associated protein essential for the regulation of cell morphology and motility. Its upregulation has been reported in pancreatic cancer [118, 119] and, was associated with poor survival among patients with renal cell carcinoma [120]. Our observation that copy number gain LOH in *PALLD* is associated with particularly poor survival is consistent with the observation in pancreatic cancer and with our prior report of an association between upregulation of alpha-actinin, another player in cytoskeleton remodeling, and poor progression-free survival among OSCC patients [121]. *DDX60L* encodes for DEAD protein with unknown function. The protein encoded by *MAML3* has been shown to be essential for Notch signaling *in vivo* [122]. Notch signaling is utilized effectively in numerous cellular and developmental processes through its multiplicity of receptors (Notch 1–4) and ligands including MAML1, MAML2 and MAML3 that serve as coactivators [123]. Notch 1 has been shown to be frequently mutated in HNSCC with nearly 40% of the 28 mutations identified predicting a truncated gene product [124]. The authors of that paper suggested that *NOTCH1* may function as a TSG rather than an oncogene in HNSCC. Our result showing having LOH in *MAML3* was associated with poor survival even in the context of copy number gains lends support to this hypothesis

Heterozygosity and partial or complete loss of Chr. 4q have been reported for verrucous hyperplasia/carcinoma [125] and HNSCC [126, 127]. Unlike the present study, that earlier report [126] on HNSCC did not find LOH on Chr. 4q to be associated with survival. While the reason for the difference is unknown, it might have to do with the fact that the earlier report was based on the examination of 33 polymorphic microsatellites while our study involved the examination of 189 LOH events.

Thus, even with a limited number of 75 patients, the current study has confirmed a number of prior findings on LOH and CNA in oral cancer as well as discovered a number of chromosomal regions that contain potential oncogenes and TSG for OSCC that warrant further investigation. Results of the current study also point to the heterogeneity and complexity of genomic alterations in OSCC and the need to take this into account when designing therapeutic interventions for oral cancer patients. Larger studies are needed to confirm or refute the observed associations of LOH, CNA, or their interactions with OSCC outcomes, and, if confirmed, to examine the clinical utility of these findings. Conducting larger studies could also discover new somatically-altered chromosomal regions that could not be detected with the multiple comparison penalties in our current study.

Supporting Information

S1 Fig. Percentage of probes showing CNA and LOH events in each OSCC. The top three plots show information for CNA normal, gain and loss. The bottom plot shows the LOH events. The 75 OSCC are sorted by the percentages of probes showing LOH events. (DOCX)

S2 Fig. Cumulative incidence curves of the OSCC-specific death for patients clustered by CNA. The left panel shows the heatmap of CNA segments across all 22 autosomes (separated by the blue dotted lines). Rows are individuals and columns are probe segments. Two patient groups resulting from hierarchical clustering are labelled with purple and blue in the color bar on the left side of the heatmap. The right panel shows the cumulative incidence curves of the OSCC-specific death for the patients in each of the two clusters. The X-axis indicates the years between surgery and last follow-up or death due to OSCC The Y-axis indicates the mortality

rate.
(DOCX)

S3 Fig. Cumulative Incidence curves of OSCC-specific death of patients clustered by LOH.
The left panel shows the heatmap of LOH across all 22 autosomes (separated by the blue dotted lines; magenta, LOH present; blue, no LOH; white, not informative). Rows are individuals and columns are probe segments. Two patient groups resulted from hierarchical clustering are labelled with magenta and blue in the color bar to the left of the heatmap. The right panel shows the Cumulative Incidence curves of OSCC-specific death of the patients in the two clusters. The X-axis indicates the years between surgery and last follow-up or death. The Y-axis indicates the mortality rate.
(DOCX)

S4 Fig. CNA and LOH data for the high-level amplification region 2 on Chr. 11 (115 probes from 11q22-24 with nucleotide position from nt99440128 to nt102804260). The top left panel shows tumor CNA data, and the color key indicates the number of copies. The bottom left panel shows the heatmap of the heatmap of LOH data (magenta, LOH present; blue, no LOH; white, not informative). In both heatmaps, the rows stand for SNPs and the columns stand for samples. Based on the CNV data, we cluster the samples into two groups (13 patients in the red group and 62 patients in the blue group) using hierarchical clustering algorithm. The right panel shows the Cumulative Incidence curves of the OSCC-specific death of the patients in the two clusters. The X-axis indicates the years between surgery and last follow-up or death. And the Y-axis indicates the mortality rate.
(DOCX)

S5 Fig. LOH and CNA data for Chr. 9p with frequent LOH event (2579 probes from nucleotide position from 36587 to 38761831). The top left panel shows the heatmap of LOH data (magenta, LOH present; blue, no LOH; white, not informative). The bottom left panel shows the heatmap of tumor CNA data, and the color key indicates the copy number. In both heatmaps, the rows stand for SNPs and the columns stand for samples. Based on the LOH data, we clustered the samples into two groups (24 patients in the magenta group and 51 patients in the blue group) using hierarchical clustering algorithm. The right panel shows the Cumulative Incidence curves of the OSCC-specific death of the patients in the two clusters. The X-axis indicates the years between surgery and last follow-up or death. The Y-axis indicates the mortality rate.
(DOCX)

S6 Fig. CNA and LOH data for the whole Chr. 4q region (8975 probes from nucleotide position from 63637813 to 183550869). The top left panel shows the heatmap of tumor CN data, and the color key indicates the copy number. The bottom left panel shows the heatmap of LOH data (magenta, LOH present; blue, no LOH; white, not informative). In both heatmaps, the rows stand for SNPs and the columns stand for samples. Based on the CNA data, we clustered the samples into two groups (15 patients in the magenta group and 60 patients in the blue group) using hierarchical clustering algorithm. The right panel shows the Cumulative Incidence curves of the OSCC-specific death of the patients in the two clusters. The X-axis indicates the years between surgery and last follow-up or death. The Y-axis indicates the mortality rate. Survival of the two clusters of patients was significantly different (p = 0.199) according to log rank test.
(DOCX)

S1 Table. Selected characteristics of HPV-negative oral squamous cell cancer patients, University of Washington Affiliated Institutions, 2004–2010 (n = 75).
(DOCX)

S2 Table. Top 100 most frequent LOH, CN gain and CN loss.
(XLSX)

S3 Table. Selected characteristics of OSCC patients according to clusters defined by genome-wide tumor CNA or LOH events, University of Washington Affiliated Institutions, 2004–2010.
(DOCX)

S4 Table. Selected characteristics for patients in clusters defined by CNA in Chr. 11, Region 1 (11q13.1–14.3, nt 68683098-nt 70375682) and Region 2 (11q22-24, nt99440128-nt102804260).
(DOCX)

S5 Table. Selected characteristics of patients in clusters defined by LOH on Chr. 9p.
(DOCX)

S6 Table. Selected characteristics for patients in clusters defined by LOH on Chr. 4q.
(DOCX)

Acknowledgments

Author Contributions

Conceived and designed the experiments: CC YZ MML MPU PL JRH DRD EM NF SMS PW. Performed the experiments: MML MPU PL JRH. Analyzed the data: CC YZ MML PL JRH DRD EM NF SMS PW. Contributed reagents/materials/analysis tools: CC YZ MPU DRD EM NF SMS PW. Wrote the paper: CC YZ MML MPU PL JRH DRD EM NF SMS PW.

References

1. Scully C, Field JK, Tanzawa H. Genetic aberrations in oral or head and neck squamous cell carcinoma 2: chromosomal aberrations. Oral Oncol. 2000; 36(4):311–27. PMID: 10899669

2. Perez-Ordonez B, Beauchemin M, Jordan RC. Molecular biology of squamous cell carcinoma of the head and neck. J Clin Pathol. 2006; 59(5):445–53. PMID: 16644882

3. Chuang SC, Scelo G, Tonita JM, Tamaro S, Jonasson JG, Kliewer EV, et al. Risk of second primary cancer among patients with head and neck cancers: A pooled analysis of 13 cancer registries. Int J Cancer. 2008; 123(10):2390–6. doi: 10.1002/ijc.23798 PMID: 18729183

4. Bockmuhl U, Schluns K, Kuchler I, Petersen S, Petersen I. Genetic imbalances with impact on survival in head and neck cancer patients. Am J Pathol. 2000; 157(2):369–75. PMID: 10934141

5. Wreesmann VB, Shi W, Thaler HT, Poluri A, Kraus DH, Pfister D, et al. Identification of novel prognosticators of outcome in squamous cell carcinoma of the head and neck. J Clin Oncol. 2004; 22 (19):3965–72. PMID: 15459219

6. Chen Y, Chen C. DNA copy number variation and loss of heterozygosity in relation to recurrence of and survival from head and neck squamous cell carcinoma: a review. Head Neck. 2008; 30 (10):1361–83. PubMed Central PMCID: PMC3220418. doi: 10.1002/hed.20861 PMID: 18642290

7. Mavros A, Hahn M, Wieland I, Koy S, Koufaki ON, Strelocke K, et al. Infrequent genetic alterations of the tumor suppressor gene PTEN/MMAC1 in squamous cell carcinoma of the oral cavity. J Oral Pathol Med. 2002; 31(5):270–6. PMID: 12110043

8. Rowley H, Jones AS, Field JK. Chromosome 18: a possible site for a tumour suppressor gene deletion in squamous cell carcinoma of the head and neck. Clin Otolaryngol Allied Sci. 1995; 20(3):266–71. PMID: 7554343

9. de Koning PJ, Bovenschen N, Leusink FK, Broekhuizen R, Quadir R, van Gemert JT, et al. Downre-gulation of SERPINB13 expression in head and neck squamous cell carcinomas associates with poor clinical outcome. Int J Cancer. 2009; 125(7):1542–50. doi: 10.1002/ijc.24507 PMID: 19569240

10. Meredith SD, Levine PA, Burns JA, Gaffey MJ, Boyd JC, Weiss LM, et al. Chromosome 11Q13 ampli-fication in head and neck squamous cell carcinoma- association with poor prognosis. Archives of Oto-laryngology—Head and Neck Surgery. 1995; 121(7):790–4. PMID: 7598859

11. Kitagawa Y, Ueda M, Ando N, Ozawa S, Shimizu N, Kitajima M. Further evidence for prognostic signif-icance of epidermal growth factor receptor gene amplification in patients with esophageal squamous cell carcinoma. Clin Cancer Res. 1996; 2(5):909–14. PMID: 9816249

12. Miyahara H, Naito H, Ueda K, Yane K, Matsunaga T, Okaichi K, et al. Amplification of int-2 and bcl-1 genes in squamous cell carcinoma of the larynx. Acta Otolaryngol. 1998; 118(5):763–8. PMID: 9840520

13. Nogueira CP, Dolan RW, Gooey J, Byahatti S, Vaughan CW, Fuleihan NS, et al. Inactivation of p53 and amplification of cyclin D1 correlate with clinical outcome in head and neck cancer. Laryngoscope. 1998; 108(3):345–50. PMID: 9504605

14. Gebhart E, Liehr T, Wolff E, Ries J, Fiedler W, Steininger H, et al. Pattern of genomic imbalances in oral squamous cell carcinomas with and without an increased copy number of 11q13. Int J Oncol. 1998; 12(5):1151–5. PMID: 9538142

15. Fujii M, Ishiguro R, Yamashita T, Tashiro M. Cyclin D1 amplification correlates with early recurrence of squamous cell carcinoma of the tongue. Cancer Lett. 2001; 172(2):187–92. PMID: 11566495

16. Singh B, Stoffel A, Gogineni S, Poluri A, Pfister DG, Shaha AR, et al. Amplification of the 3q26.3 locus is associated with progression to invasive cancer and is a negative prognostic factor in head and neck squamous cell carcinomas. Am J Pathol. 2002; 161(2):365–71. PMID: 12163360

17. Namazie A, Alavi S, Olopade OI, Pauletti G, Aghamohammadi N, Aghamohammadi M, et al. Cyclin D1 amplification and p16(MTS1/CDK4I) deletion correlate with poor prognosis in head and neck tumors. Laryngoscope. 2002; 112(3):472–81. PMID: 12148857

18. Reis PP, Rogatto SR, Kowalski LP, Nishimoto IN, Montovani JC, Corpus G, et al. Quantitative real-time PCR identifies a critical region of deletion on 22q13 related to prognosis in oral cancer. Onco-gene. 2002; 21(42):6480–7. PMID: 12226751

19. Miyamoto R, Uzawa N, Nagaoka S, Hirata Y, Amagasa T. Prognostic significance of cyclin D1 amplifi-cation and overexpression in oral squamous cell carcinomas. Oral Oncol. 2003; 39(6):610–8. PMID: 12798405

20. Akervall J, Bockmuhl U, Petersen I, Yang K, Carey TE, Kurnit DM. The gene ratios c-MYC:cyclin-dependent kinase (CDK)N2A and CCND1:CDKN2A correlate with poor prognosis in squamous cell carcinoma of the head and neck. Clin Cancer Res. 2003; 9(5):1750–5. PMID: 12738730

21. Fujita Y, Sakakura C, Shimomura K, Nakanishi M, Yasuoka R, Aragane H, et al. Chromosome arm 20q gains and other genomic alterations in esophageal squamous cell carcinoma, as analyzed by comparative genomic hybridization and fluorescence in situ hybridization. Hepatogastroenterology. 2003; 50(54):1857–63. PMID: 14696419

22. Sticht C, Hofele C, Flechtenmacher C, Bosch FX, Freier K, Lichter P, et al. Amplification of Cyclin L1 is associated with lymph node metastases in head and neck squamous cell carcinoma (HNSCC). Br J Cancer. 2005; 92(4):770–4. PMID: 15700036

23. Chung CH, Ely K, McGavran L, Varella-Garcia M, Parker J, Parker N, et al. Increased epidermal growth factor receptor gene copy number is associated with poor prognosis in head and neck squa-mous cell carcinomas. J Clin Oncol. 2006; 24(25):4170–6. PMID: 16943533

24. Sabbir MG, Dasgupta S, Roy A, Bhoumik A, Dam A, Roychoudhury S, et al. Genetic alterations (amplification and rearrangement) of D-type cyclins loci in head and neck squamous cell carcinoma of Indian patients: prognostic significance and clinical implications. DiagnMolPathol. 2006; 15(1):7–16.

25. Smeets SJ, Braakhuis BJ, Abbas S, Snijders PJ, Ylstra B, van de Wiel MA, et al. Genome-wide DNA copy number alterations in head and neck squamous cell carcinomas with or without oncogene-expressing human papillomavirus. Oncogene. 2006; 25(17):2558–64. PMID: 16314836

26. Ashman JN, Patmore HS, Condon LT, Cawkwell L, Stafford ND, Greenman J. Prognostic value of genomic alterations in head and neck squamous cell carcinoma detected by comparative genomic hybridisation. Br J Cancer. 2003; 89(5):864–9. PMID: 12942119

27. Gebhart E, Ries J, Wiltfang J, Liehr T, Efferth T. Genomic gain of the epidermal growth factor receptor harboring band 7p12 is part of a complex pattern of genomic imbalances in oral squamous cell carcinomas. Arch Med Res. 2004; 35(5):385–94. PMID: 15610907

28. LaFramboise T, Weir BA, Zhao X, Beroukhim R, Li C, Harrington D, et al. Allele-specific amplification in cancer revealed by SNP array analysis. PLoS Comput Biol. 2005; 1(6):e65. PMID: 16322765

29. Dutt A, Beroukhim R. Single nucleotide polymorphism array analysis of cancer. Curr Opin Oncol. 2006; 19(1):43–9.

30. Chen C, Mendez E, Houck J, Fan W, Lohavanichbutr P, Doody D, et al. Gene expression profiling identifies genes predictive of oral squamous cell carcinoma. Cancer Epidemiol Biomarkers Prev. 2008; 17(8):2152–62. PubMed Central PMCID: PMC2575803. doi: 10.1158/1055-9965.EPI-07-2893 PMID: 18669583

31. Lohavanichbutr P, Houck J, Fan W, Yueh B, Mendez E, Futran N, et al. Genomewide gene expression profiles of HPV-positive and HPV-negative oropharyngeal cancer: potential implications for treatment choices. Archives of Otolaryngology—Head and Neck Surgery. 2009; 135(2):180–8. PubMed Central PMCID: PMC2761829. doi: 10.1001/archoto.2008.540 PMID: 19221247

32. Miller SA, Dykes DD, Polesky HF. A simple salting out procedure for extracting DNA from human nucleated cells. Nucleic Acids Res. 1988; 16:1215. PMID: 3344216

33. Bengtsson H, Wirapati P, Speed TP. A single-array preprocessing method for estimating full-resolution raw copy numbers from all Affymetrix genotyping arrays including GenomeWideSNP 5 & 6. Bioinformatics. 2009; 25(17):2149–56. PubMed Central PMCID: PMC2734319. doi: 10.1093/bioinformatics/btp371 PMID: 19535535

34. Chen H, Xing H, Zhang NR. Stochastic segmentation models for allele-specific copy number estimation with SNP-array data. PLoS Comput Biol. 2011; 7(1):e1001060. doi: 10.1371/journal.pcbi.1001060 PMID: 21298078

35. Storey JD. A direct approach to false discovery rates. J Roy Stat Soc Ser B (Stat Method). 2002; 64(3):479–98. doi: 10.1111/1467-9868.00346

36. Toguchida J, Yamaguchi T, Dayton SH, Beauchamp RL, Herrera GE, Ishizaki K, et al. Prevalence and spectrum of germline mutations of the p53 gene among patients with sarcoma. N Engl J Med. 1992; 326(20):1301–8. PMID: 1565143

37. Partridge M, Kiguwa S, Langdon JD. Frequent deletion of chromosome 3p in oral squamous cell carcinoma. Eur J Cancer B Oral Oncol. 1994; 30B(4):248–51. Epub 1994/07/01. PMID: 7950839.

38. El-Naggar AK, Hurr K, Batsakis JG, Luna MA, Goepfert H, Huff V. Sequential loss of heterozygosity at microsatellite motifs in preinvasive and invasive head and neck squamous carcinoma. Cancer Res. 1995; 55(12):2656–9. PMID: 7780981

39. Field JK, Kiaris H, Risk JM, Tsiriyotis C, Adamson R, Zoumpourlis V, et al. Allelotype of squamous cell carcinoma of the head and neck: fractional allele loss correlates with survival. Br J Cancer. 1995; 72(5):1180–8. Epub 1995/11/01. PMID: 7577465; PubMed Central PMCID: PMCPMC2033926.

40. Ishwad CS, Ferrell RE, Rossie KN, Appel BN, Johnson JT, Myers EN, et al. Loss of heterozygosity of the short arm of chromosomes 3 and 9 in oral cancer. Int J Cancer. 1996; 69(1):1–4. PMID: 8600052

41. Waber PG, Lee NK, Nisen PD. Frequent allelic loss at chromosome arm 3p is distinct from genetic alterations of the Von-Hippel Lindau tumor suppressor gene in head and neck cancer. Oncogene. 1996; 12(2):365–9. PMID: 8570213

42. Waber P, Dlugosz S, Cheng QC, Truelson J, Nisen PD. Genetic alterations of chromosome band 9p21-22 in head and neck cancer are not restricted to p16INK4a. Oncogene. 1997; 15(14):1699–704. PMID: 9349503

43. Lydiatt WM, Davidson BJ, Schantz SP, Caruana S, Chaganti RS. 9p21 deletion correlates with recurrence in head and neck cancer. Head Neck. 1998; 20(2):113–8. PMID: 9484941

44. Nakanishi H, Wang XL, Imai FL, Kato J, Shiiba M, Miya T, et al. Localization of a novel tumor suppressor gene loci on chromosome 9p21-22 in oral cancer. Anticancer Res. 1999; 19(1A):29–34. PMID: 10226521

45. Blons H, Cabelguenne A, Carnot F, Laccourreye O, de Waziers I, Hamelin R, et al. Microsatellite analysis and response to chemotherapy in head-and-neck squamous-cell carcinoma. Int J Cancer. 1999; 84(4):410–5. PMID: 10404095

46. Huang MF, Chang YC, Liao PS, Huang TH, Tsay CH, Chou MY. Loss of heterozygosity of p53 gene of oral cancer detected by exfoliative cytology. Oral Oncol. 1999; 35(3):296–301. PMID: 10621851

47. Nunn J, Scholes AG, Liloglou T, Nagini S, Jones AS, Vaughan ED, et al. Fractional allele loss indicates distinct genetic populations in the development of squamous cell carcinoma of the head and neck (SCCHN). Carcinogenesis. 1999; 20(12):2219–28. Epub 1999/12/11. PMID: 10590212.

48. Ng IO, Xiao L, Lam KY, Yuen PW, Ng M. Microsatellite alterations in squamous cell carcinoma of the head and neck—clustering of loss of heterozygosity in a distinct subset. Oral Oncol. 2000; 36(5):484–90. PMID: 10964058

49. Miracca EC, Yamamoto L, Contado D, de Souza Silva Takimoto M, Kowalski LP, Nagai MA. Distinct chromosomal deleted regions defining different subsets of head and neck tumors. Diagn Mol Pathol. 2000; 9(4):229–33. PMID: 11129447

50. Martinez A, Walker RA, Shaw JA, Dearing SJ, Maher ER, Latif F. Chromosome 3p allele loss in early invasive breast cancer: detailed mapping and association with clinicopathological features. Mol Pathol. 2001; 54(5):300–6. PubMed Central PMCID: PMC1187086. PMID: 11577171

51. Gotte K, Riedel F, Neubauer J, Schafer C, Coy JF, Hormann K. The relationship between allelic imbalance on 17p, p53 mutation and p53 overexpression in head and neck cancer. Int J Oncol. 2001; 19 (2):331–6. PMID: 11445847

52. Kayahara H, Yamagata H, Tanioka H, Miki T, Hamakawa H. Frequent loss of heterozygosity at 3p25-p26 is associated with invasive oral squamous cell carcinoma. J Hum Genet. 2001; 46(6):335–41. PMID: 11393537

53. Arai K, Shibahara T, Yamamoto N, Yakushiji T, Tanaka C, Noma H. Frequent allelic loss/imbalance on the short arm of chromosome 3 in tongue cancer. Bull Tokyo Dent Coll. 2001; 42(3):151–7. Epub 2002/01/25. PMID: 11806149.

54. Arai K, Shibahara T, Yamamoto N, Noma H. The presence of candidate tumor suppressor gene loci at chromosome 3p for oral squamous cell carcinomas. Oral Oncology. 2002; 38(8):763–71. PMID: 12570055

55. Hogg RP, Honorio S, Martinez A, Agathanggelou A, Dallol A, Fullwood P, et al. Frequent 3p allele loss and epigenetic inactivation of the RASSF1A tumour suppressor gene from region 3p21.3 in head and neck squamous cell carcinoma. Eur J Cancer. 2002; 38(12):1585–92. Epub 2002/07/27. PMID: 12142046.

56. Beder LB, Gunduz M, Ouchida M, Fukushima K, Gunduz E, Ito S, et al. Genome-wide analyses on loss of heterozygosity in head and neck squamous cell carcinomas. Lab Invest. 2003; 83(1):99–105. PMID: 12533690

57. Schneider-Stock R, Mawrin C, Motsch C, Boltze C, Peters B, Hartig R, et al. Retention of the arginine allele in codon 72 of the p53 gene correlates with poor apoptosis in head and neck cancer. Am J Pathol. 2004; 164(4):1233–41. PubMed Central PMCID: PMC1615339. PMID: 15039212

58. Tran TN, Liu Y, Takagi M, Yamaguchi A, Fujii H. Frequent promoter hypermethylation of RASSF1A and p16INK4a and infrequent allelic loss other than 9p21 in betel-associated oral carcinoma in a Vietnamese non-smoking/non-drinking female population. J Oral Pathol Med. 2005; 34(3):150–6. PMID: 15689228

59. Yamamoto N, Kuroiwa T, Katakura A, Shibahara T, Choudhury C. Loss of heterozygosity (LOH) on chromosomes 2q, 3p and 21q in Indian oral squamous cell carcinoma. Bull Tokyo Dent Coll. 2007; 48 (3):109–17. PMID: 18057857

60. Koy S, Plaschke J, Luksch H, Friedrich K, Kuhlisch E, Eckelt U, et al. Microsatellite instability and loss of heterozygosity in squamous cell carcinoma of the head and neck. Head Neck. 2008; 30(8):1105–13. doi: 10.1002/hed.20857 PMID: 18615731

61. Lazar AD, Winter MR, Nogueira CP, Larson PS, Finnemore EM, Dolan RW, et al. Loss of heterozygosity at 11q23 in squamous cell carcinoma of the head and neck is associated with recurrent disease. Clin Cancer Res. 1998; 4(11):2787–93. PMID: 9829743

62. Lee DJ, Schonleben F, Banuchi VE, Qiu W, Close LG, Assaad AM, et al. Multiple tumor-suppressor genes on chromosome 3p contribute to head and neck squamous cell carcinoma tumorigenesis. Cancer Biol Ther. 2010; 10(7):689–93. Epub 2010/07/27. doi: 10.4161/cbt.10.7.12886 PMID: 20657180; PubMed Central PMCID: PMCPMC3093810.

63. Sjoblom T, Jones S, Wood LD, Parsons DW, Lin J, Barber TD, et al. The consensus coding sequences of human breast and colorectal cancers. Science. 2006; 314(5797):268–74. Epub 2006/ 09/09. doi: 10.1126/science.1133427 PMID: 16959974.

64. Cloos PA, Christensen J, Agger K, Maiolica A, Rappsilber J, Antal T, et al. The putative oncogene GASC1 demethylates tri- and dimethylated lysine 9 on histone H3. Nature. 2006; 442(7100):307–11. Epub 2006/05/30. doi: 10.1038/nature04837 PMID: 16732293.

65. Young LC, Hendzel MJ. The oncogenic potential of Jumonji D2 (JMJD2/KDM4) histone demethylase overexpression. Biochem Cell Biol. 2013; 91(6):369–77. Epub 2013/11/14. doi: 10.1139/bcb-2012-0054 PMID: 24219278.

66. Chen SF, Nieh S, Jao SW, Wu MZ, Liu CL, Chang YC, et al. The paracrine effect of cancer-associated fibroblast-induced interleukin-33 regulates the invasiveness of head and neck squamous cell carcinoma. J Pathol. 2013; 231(2):180–9. Epub 2013/06/19. doi: 10.1002/path.4226 PMID: 23775566.

67. Veeriah S, Brennan C, Meng S, Singh B, Fagin JA, Solit DB, et al. The tyrosine phosphatase PTPRD is a tumor suppressor that is frequently inactivated and mutated in glioblastoma and other human cancers. Proc Natl Acad Sci U S A. 2009; 106(23):9435–40. Epub 2009/05/30. doi: 10.1073/pnas.0900571106 PMID: 19478061; PubMed Central PMCID: PMCPMC2687998.

68. Kohno T, Otsuka A, Girard L, Sato M, Iwakawa R, Ogiwara H, et al. A catalog of genes homozygously deleted in human lung cancer and the candidacy of PTPRD as a tumor suppressor gene. Genes Chromosomes Cancer. 2010; 49(4):342–52. Epub 2010/01/15. doi: 10.1002/gcc.20746 PMID: 20073072; PubMed Central PMCID: PMCPMC2921682.

69. Giefing M, Zemke N, Brauze D, Kostrzewska-Poczekaj M, Luczak M, Szaumkessel M, et al. High resolution ArrayCGH and expression profiling identifies PTPRD and PCDH17/PCH68 as tumor suppressor gene candidates in laryngeal squamous cell carcinoma. Genes Chromosomes Cancer. 2011; 50 (3):154–66. Epub 2011/01/08. doi: 10.1002/gcc.20840 PMID: 21213369.

70. Kathiresan S, Willer CJ, Peloso GM, Demissie S, Musunuru K, Schadt EE, et al. Common variants at 30 loci contribute to polygenic dyslipidemia. Nat Genet. 2009; 41(1):56–65. Epub 2008/12/09. doi: 10.1038/ng.291 PMID: 19060906; PubMed Central PMCID: PMCPMC2881676.

71. Teslovich TM, Musunuru K, Smith AV, Edmondson AC, Stylianou IM, Koseki M, et al. Biological, clinical and population relevance of 95 loci for blood lipids. Nature. 2010; 466(7307):707–13. Epub 2010/08/06. doi: 10.1038/nature09270 PMID: 20686565; PubMed Central PMCID: PMCPMC3039276.

72. Fu WN, Shang C, Huang DF, Xu ZM, Sun XH, Sun KL. Average-12.9 chromosome imbalances coupling with 15 differential expression genes possibly involved in the carcinogenesis, progression and metastasis of supraglottic laryngeal squamous cell cancer. Zhonghua Yi Xue Yi Chuan Xue Za Zhi. 2006; 23(1):7–11. Epub 2006/02/04. PMID: 16456776.

73. Shang C, Guo Y, Fu S, Fu W, Sun K. SH3GL2 gene participates in MEK-ERK signal pathway partly by regulating EGFR in the laryngeal carcinoma cell line Hep2. Med Sci Monit. 2010; 16(6):BR168–73. Epub 2010/06/01. PMID: 20512084.

74. Smyth I, Du X, Taylor MS, Justice MJ, Beutler B, Jackson IJ. The extracellular matrix gene Frem1 is essential for the normal adhesion of the embryonic epidermis. Proc Natl Acad Sci U S A. 2004; 101 (37):13560–5. Epub 2004/09/04. doi: 10.1073/pnas.0402760101 PMID: 15345741; PubMed Central PMCID: PMCPMC518794.

75. Qiu W, Schonleben F, Li X, Su GH. Disruption of transforming growth factor beta-Smad signaling pathway in head and neck squamous cell carcinoma as evidenced by mutations of SMAD2 and SMAD4. Cancer Lett. 2007; 245(1–2):163–70. Epub 2006/02/16. doi: 10.1016/j.canlet.2006.01.003 PMID: 16478646; PubMed Central PMCID: PMCPMC1741856.

76. Nakao A, Imamura T, Souchelnytskyi S, Kawabata M, Ishisaki A, Oeda E, et al. TGF-beta receptor-mediated signalling through Smad2, Smad3 and Smad4. EMBO J. 1997; 16(17):5353–62. Epub 1997/10/06. doi: 10.1093/emboj/16.17.5353 PMID: 9311995; PubMed Central PMCID: PMCPMC1170167.

77. Temam S, Kawaguchi H, El-Naggar AK, Jelinek J, Tang H, Liu DD, et al. Epidermal growth factor receptor copy number alterations correlate with poor clinical outcome in patients with head and neck squamous cancer. J Clin Oncol. 2007; 25(16):2164–70. PMID: 17538160

78. Bandres E, Barricarte R, Cantero C, Honorato B, Malumbres R, Zarate R, et al. Epidermal growth factor receptor (EGFR) polymorphisms and survival in head and neck cancer patients. Oral Oncol. 2007; 43(7):713–9. Epub 2006/11/23. doi: 10.1016/j.oraloncology.2006.09.002 PMID: 17112774.

79. Hama T, Yuza Y, Saito Y, Ou J, Kondo S, Okabe M, et al. Prognostic significance of epidermal growth factor receptor phosphorylation and mutation in head and neck squamous cell carcinoma. Oncologist. 2009; 14(9):900–8. Epub 2009/09/04. doi: 10.1634/theoncologist.2009-0058 PMID: 19726454.

80. Takebayashi S, Ogawa T, Jung KY, Muallem A, Mineta H, Fisher SG, et al. Identification of new minimally lost regions on 18q in head and neck squamous cell carcinoma. Cancer Res. 2000; 60 (13):3397–403. Epub 2000/07/26. PMID: 10910046.

81. Bornstein S, White R, Malkoski S, Oka M, Han G, Cleaver T, et al. Smad4 loss in mice causes spontaneous head and neck cancer with increased genomic instability and inflammation. J Clin Invest. 2009; 119(11):3408–19. Epub 2009/10/21. doi: 10.1172/jci38854 PMID: 19841536; PubMed Central PMCID: PMCPMC2769185.

82. Malkoski SP, Wang XJ. Two sides of the story? Smad4 loss in pancreatic cancer versus head-and-neck cancer. FEBS Lett. 2012; 586(14):1984–92. Epub 2012/02/11. doi: 10.1016/j.febslet.2012.01.054 PMID: 22321641; PubMed Central PMCID: PMCPMC3285395.

83. Kim SK, Fan Y, Papadimitrakopoulou V, Clayman G, Hittelman WN, Hong WK, et al. DPC4, a candidate tumor suppressor gene, is altered infrequently in head and neck squamous cell carcinoma. Cancer Res. 1996; 56(11):2519–21. Epub 1996/06/01. PMID: 8653689.

84. Ribeiro IP, Marques F, Caramelo F, Ferrao J, Prazeres H, Juliao MJ, et al. Genetic imbalances detected by multiplex ligation-dependent probe amplification in a cohort of patients with oral squamous cell carcinoma-the first step towards clinical personalized medicine. Tumour Biol. 2014; 35 (5):4687–95. Epub 2014/01/31. doi: 10.1007/s13277-014-1614-9 PMID: 24477574.

85. Nishikawa Y, Miyazaki T, Nakashiro K, Yamagata H, Isokane M, Goda H, et al. Human FAT1 cadherin controls cell migration and invasion of oral squamous cell carcinoma through the localization of beta-catenin. Oncol Rep. 2011; 26(3):587–92. Epub 2011/05/28. doi: 10.3892/or.2011.1324 PMID: 21617878.

86. Mountzios G, Rampias T, Psyrri A. The mutational spectrum of squamous-cell carcinoma of the head and neck: Targetable genetic events and clinical impact. Ann Oncol. 2014. Epub 2014/04/11. doi: 10.1093/annonc/mdu143 PMID: 24718888.

87. Nakaya K, Yamagata HD, Arita N, Nakashiro KI, Nose M, Miki T, et al. Identification of homozygous deletions of tumor suppressor gene FAT in oral cancer using CGH-array. Oncogene. 2007; 26 (36):5300–8. PMID: 17325662

88. Katoh M, Katoh M. FLJ10261 gene, located within the CCND1-EMS1 locus on human chromosome 11q13, encodes the eight-transmembrane protein homologous to C12orf3, C11orf25 and FLJ34272 gene products. Int J Oncol. 2003; 22(6):1375–81. PMID: 12739008

89. Freier K, Sticht C, Hofele C, Flechtenmacher C, Stange D, Puccio L, et al. Recurrent coamplification of cytoskeleton-associated genes EMS1 and SHANK2 with CCND1 in oral squamous cell carcinoma. Genes, Chromosomes and Cancer. 2006; 45(2):118–25. PMID: 16235239

90. Chen YJ, Lin SC, Kao T, Chang CS, Hong PS, Shieh TM, et al. Genome-wide profiling of oral squamous cell carcinoma. J Pathol. 2004; 204(3):326–32. PMID: 15372456

91. Katoh M, Katoh M. Comparative genomics on mammalian Fgf3-Fgf4 locus. Int J Oncol. 2005; 27 (1):281–5. Epub 2005/06/09. PMID: 15942670.

92. Jin C, Jin Y, Gisselsson D, Wennerberg J, Wah TS, Stromback B, et al. Molecular cytogenetic characterization of the 11q13 amplicon in head and neck squamous cell carcinoma. Cytogenet Cell Genet. 2006; 115(2):99–106.

93. Sugahara K, Michikawa Y, Ishikawa K, Shoji Y, Iwakawa M, Shibahara T, et al. Combination effects of distinct cores in 11q13 amplification region on cervical lymph node metastasis of oral squamous cell carcinoma. Int J Oncol. 2011; 39(4):761–9. Epub 2011/06/28. doi: 10.3892/ijo.2011.1094 PMID: 21701773.

94. Ying J, Shan L, Li J, Zhong L, Xue L, Zhao H, et al. Genome-wide screening for genetic alterations in esophageal cancer by aCGH identifies 11q13 amplification oncogenes associated with nodal metastasis. PLoS One. 2012; 7(6):e39797. Epub 2012/07/05. doi: 10.1371/journal.pone.0039797 PMID: 22761904; PubMed Central PMCID: PMCPMC3382571.

95. Ribeiro IP, Marques F, Caramelo F, Pereira J, Patricio M, Prazeres H, et al. Genetic gains and losses in oral squamous cell carcinoma: impact on clinical management. Cell Oncol (Dordr). 2014; 37(1):29–39. Epub 2013/12/20. doi: 10.1007/s13402-013-0161-5 PMID: 24353162.

96. Janssen JW, Imoto I, Inoue J, Shimada Y, Ueda M, Imamura M, et al. MYEOV, a gene at 11q13, is coamplified with CCND1, but epigenetically inactivated in a subset of esophageal squamous cell carcinomas. J Hum Genet. 2002; 47(9):460–4. PMID: 12202983

97. Iizuka S, Ishimaru N, Kudo Y. Matrix metalloproteinases: the gene expression signatures of head and neck cancer progression. Cancers (Basel). 2014; 6(1):396–415. Epub 2014/02/18. doi: 10.3390/cancers6010396 PMID: 24531055; PubMed Central PMCID: PMCPMC3980592.

98. Snijders AM, Schmidt BL, Fridlyand J, Dekker N, Pinkel D, Jordan RC, et al. Rare amplicons implicate frequent deregulation of cell fate specification pathways in oral squamous cell carcinoma. Oncogene. 2005; 24(26):4232–42. Epub 2005/04/13. doi: 10.1038/sj.onc.1208601 PMID: 15824737.

99. Li SY, Hu JA, Wang HM. Expression of Yes-associated protein 1 gene and protein in oral squamous cell carcinoma. Chin Med J (Engl). 2013; 126(4):655–8. Epub 2013/02/21. PMID: 23422184.

100. Bernaldo de Quiros S, Merlo A, Secades P, Zambrano I, de Santa Maria IS, Ugidos N, et al. Identification of TRPC6 as a possible candidate target gene within an amplicon at 11q21-q22.2 for migratory capacity in head and neck squamous cell carcinomas. BMC Cancer. 2013; 13:116. Epub 2013/03/19. doi: 10.1186/1471-2407-13-116 PMID: 23497198; PubMed Central PMCID: PMCPMC3606258.

101. Ding X, He Z, Zhou K, Cheng J, Yao H, Lu D, et al. Essential role of TRPC6 channels in G2/M phase transition and development of human glioma. J Natl Cancer Inst. 2010; 102(14):1052–68. Epub 2010/06/18. doi: 10.1093/jnci/djq217 PMID: 20554944.

102. Chigurupati S, Venkataraman R, Barrera D, Naganathan A, Madan M, Paul L, et al. Receptor channel TRPC6 is a key mediator of Notch-driven glioblastoma growth and invasiveness. Cancer Res. 2010; 70(1):418–27. Epub 2009/12/24. doi: 10.1158/0008-5472.can-09-2654 PMID: 20028870.

103. Dhennin-Duthille I, Gautier M, Faouzi M, Guilbert A, Brevet M, Vaudry D, et al. High expression of transient receptor potential channels in human breast cancer epithelial cells and tissues: correlation with pathological parameters. Cell Physiol Biochem. 2011; 28(5):813–22. Epub 2011/12/20. doi: 10.1159/000335795 PMID: 22178934.

104. Song J, Wang Y, Li X, Shen Y, Yin M, Guo Y, et al. Critical role of TRPC6 channels in the development of human renal cell carcinoma. Mol Biol Rep. 2013; 40(8):5115–22. Epub 2013/05/24. doi: 10.1007/s11033-013-2613-4 PMID: 23700295.

105. Zhang SS, Wen J, Yang F, Cai XL, Yang H, Luo KJ, et al. High expression of transient potential receptor C6 correlated with poor prognosis in patients with esophageal squamous cell carcinoma. Medical oncology (Northwood, London, England). 2013; 30(3):607. Epub 2013/05/21. doi: 10.1007/s12032-013-0607-7 PMID: 23686700.

106. Binmadi NO, Yang YH, Zhou H, Proia P, Lin YL, De Paula AM, et al. Plexin-B1 and semaphorin 4D cooperate to promote perineural invasion in a RhoA/ROK-dependent manner. Am J Pathol. 2012; 180 (3):1232–42. Epub 2012/01/19. doi: 10.1016/j.ajpath.2011.12.009 PMID: 22252234; PubMed Central PMCID: PMCPMC3349891.

107. Takekoshi T, Tada Y, Watanabe T, Sugaya M, Hoashi T, Komine M, et al. Identification of a novel marker for dendritic cell maturation, mouse transmembrane protein 123. J Biol Chem. 2010; 285 (41):31876–84. Epub 2010/08/06. doi: 10.1074/jbc.M110.118877 PMID: 20685650; PubMed Central PMCID: PMCPMC2951259.

108. Hess CJ, Berkhof J, Denkers F, Ossenkoppele GJ, Schouten JP, Oudejans JJ, et al. Activated intrinsic apoptosis pathway is a key related prognostic parameter in acute myeloid leukemia. J Clin Oncol. 2007; 25(10):1209–15. Epub 2007/04/03. doi: 10.1200/jco.2006.08.4061 PMID: 17401010.

109. Bashyam MD, Bair R, Kim YH, Wang P, Hernandez-Boussard T, Karikari CA, et al. Array-based comparative genomic hybridization identifies localized DNA amplifications and homozygous deletions in pancreatic cancer. Neoplasia. 2005; 7(6):556–62. Epub 2005/07/23. PMID: 16036106; PubMed Central PMCID: PMCPMC1501288.

110. Guo W, Li GJ, Xu HB, Xie JS, Shi TP, Zhang SZ, et al. In vitro biological characterization of DCUN1D5 in DNA damage response. Asian Pac J Cancer Prev. 2012; 13(8):4157–62. Epub 2012/10/27. PMID: 23098533.

111. Drake AC, Khoury M, Leskov I, Iliopoulou BP, Fragoso M, Lodish H, et al. Human CD34+ CD133+ hematopoietic stem cells cultured with growth factors including Angptl5 efficiently engraft adult NOD-SCID Il2rgamma-/- (NSG) mice. PLoS One. 2011; 6(4):e18382. Epub 2011/05/12. doi: 10.1371/journal.pone.0018382 PMID: 21559522; PubMed Central PMCID: PMCPMC3084708.

112. Turner N, Grose R. Fibroblast growth factor signalling: from development to cancer. Nat Rev Cancer. 2010; 10(2):116–29. Epub 2010/01/23. doi: 10.1038/nrc2780 PMID: 20094046.

113. Tsui IF, Poh CF, Garnis C, Rosin MP, Zhang L, Lam WL. Multiple pathways in the FGF signaling network are frequently deregulated by gene amplification in oral dysplasias. Int J Cancer. 2009; 125 (9):2219–28. Epub 2009/07/23. doi: 10.1002/ijc.24611 PMID: 19623652; PubMed Central PMCID: PMCPMC2761835.

114. Hyeon J, Ahn S, Lee JJ, Song DH, Park CK. Expression of fibroblast growth factor 19 is associated with recurrence and poor prognosis of hepatocellular carcinoma. Dig Dis Sci. 2013; 58(7):1916–22. Epub 2013/03/05. doi: 10.1007/s10620-013-2609-x PMID: 23456506.

115. Daniele G, Corral J, Molife LR, de Bono JS. FGF receptor inhibitors: role in cancer therapy. Curr Oncol Rep. 2012; 14(2):111–9. Epub 2012/02/09. doi: 10.1007/s11912-012-0225-0 PMID: 22311684.

116. Beenken A, Mohammadi M. The FGF family: biology, pathophysiology and therapy. Nat Rev Drug Discov. 2009; 8(3):235–53. Epub 2009/02/28. doi: 10.1038/nrd2792 PMID: 19247306; PubMed Central PMCID: PMCPMC3684054.

117. Lou JY, Laezza F, Gerber BR, Xiao M, Yamada KA, Hartmann H, et al. Fibroblast growth factor 14 is an intracellular modulator of voltage-gated sodium channels. J Physiol. 2005; 569(Pt 1):179–93. Epub 2005/09/17. doi: 10.1113/jphysiol.2005.097220 PMID: 16166153; PubMed Central PMCID: PMCPMC1464207.

118. Pogue-Geile KL, Chen R, Bronner MP, Crnogorac-Jurcevic T, Moyes KW, Dowen S, et al. Palladin mutation causes familial pancreatic cancer and suggests a new cancer mechanism. PLoS Med. 2006; 3(12):e516. Epub 2006/12/30. doi: 10.1371/journal.pmed.0030516 PMID: 17194196; PubMed Central PMCID: PMCPMC1751121.

119. Goicoechea SM, Garcia-Mata R, Staub J, Valdivia A, Sharek L, McCulloch CG, et al. Palladin promotes invasion of pancreatic cancer cells by enhancing invadopodia formation in cancer-associated

fibroblasts. Oncogene. 2014; 33(10):1265–73. Epub 2013/03/26. doi: 10.1038/onc.2013.68 PMID: 23524582; PubMed Central PMCID: PMCPMC3912215.

120. Gupta V, Bassi DE, Simons JD, Devarajan K, Al-Saleem T, Uzzo RG, et al. Elevated expression of stromal palladin predicts poor clinical outcome in renal cell carcinoma. PLoS One. 2011; 6(6):e21494. Epub 2011/07/09. doi: 10.1371/journal.pone.0021494 PMID: 21738681; PubMed Central PMCID: PMCPMC3125241.

121. Lohavanichbutr P, Houck J, Doody DR, Wang P, Mendez E, Futran N, et al. Gene expression in uninvolved oral mucosa of OSCC patients facilitates identification of markers predictive of OSCC outcomes. PLoS One. 2012; 7(9):e46575. PubMed Central PMCID: PMC3460916. doi: 10.1371/journal.pone.0046575 PMID: 23029552

122. Oyama T, Harigaya K, Sasaki N, Okamura Y, Kokubo H, Saga Y, et al. Mastermind-like 1 (MamL1) and mastermind-like 3 (MamL3) are essential for Notch signaling in vivo. Development. 2011; 138 (23):5235–46. Epub 2011/11/10. doi: 10.1242/dev.062802 PMID: 22069191.

123. Wu L, Sun T, Kobayashi K, Gao P, Griffin JD. Identification of a family of mastermind-like transcriptional coactivators for mammalian notch receptors. Mol Cell Biol. 2002; 22(21):7688–700. PubMed Central PMCID: PMC135662. PMID: 12370315

124. Agrawal N, Frederick MJ, Pickering CR, Bettegowda C, Chang K, Li RJ, et al. Exome sequencing of head and neck squamous cell carcinoma reveals inactivating mutations in NOTCH1. Science. 2011; 333(6046):1154–7. PubMed Central PMCID: PMC3162986. doi: 10.1126/science.1206923 PMID: 21798897

125. Poh CF, Zhang L, Lam WL, Zhang X, An D, Chau C, et al. A high frequency of allelic loss in oral verrucous lesions may explain malignant risk. Lab Invest. 2001; 81:629–34. PMID: 11304582

126. Shah SI, Yip L, Greenberg B, Califano JA, Chow J, Eisenberger CF, et al. Two distinct regions of loss on chromosome arm 4q in primary head and neck squamous cell carcinoma. Archives of Otolaryngology—Head and Neck Surgery. 2000; 126(9):1073–6. PMID: 10979119

127. Koch WM, Lango M, Sewell D, Zahurak M, Sidransky D. Head and neck cancer in nonsmokers: a distinct clinical and molecular entity. Laryngoscope. 1999; 109(10):1544–51. PMID: 10522920